

Alteration Detection of Tensor Dependence Structure via Sparsity-Exploited Reranking Algorithm

Li Ma[†], Shenghao Qin[†], and Yin Xia[†]

[†]*Department of Statistics and Data Science, Fudan University*

Abstract

Tensor-valued data arise frequently from a wide variety of scientific applications, and many among them can be translated into an alteration detection problem of tensor dependence structures. In this article, we formulate the problem under the popularly adopted tensor-normal distributions and aim at two-sample correlation/partial correlation comparisons of tensor-valued observations. Through decorrelation and centralization, a separable covariance structure is employed to pool sample information from different tensor modes to enhance the power of the test. Additionally, we propose a novel **S**parsity-**E**xploited **R**eranking **A**lgorithm (SERA) to further improve the multiple testing efficiency. The algorithm is approached through reranking of the p -values derived from the primary test statistics, by incorporating a carefully constructed auxiliary tensor sequence. Besides the tensor framework, SERA is also generally applicable to a wide range of two-sample large-scale inference problems with sparsity structures, and is of independent interest. The asymptotic properties of the proposed test are derived and the algorithm is shown to control the false discovery at the pre-specified level. We demonstrate the efficacy of the proposed method through intensive simulations and two scientific applications.

Keywords: False discovery rate, Multiple testing, Tensor normal, Separable covariance, Weighted p -values.

1 Introduction

The growing accessibility of multi-dimensional data has attracted increasing attention to tensor inference. Tensors are higher-order parallels of vectors (first-order) and matrices (second-order), and are denoted by bold Euler letters such as \mathbf{Y} throughout the paper. Specifically, a K -th order tensor with dimension vector (m_1, \dots, m_K) is denoted by $\mathbf{Y} \in \mathbb{R}^{m_1 \times m_2 \times \dots \times m_K}$, and it has K “modes” in total (Hoff, 2011). As a concrete example, the international trade dataset in Section 5.1 collects monthly imports of 97 commodity types over 30 countries from the year 2015 to 2022. The data from each year is a $97 \times 30 \times 12$ tensor-valued observation, where the commodity types, countries and months serve as the first, second and third mode, respectively. Besides, tensor-valued data also arise in many other fields, including climate change detection (e.g., the analysis in Section 5.2), gene microarray study (Zahn et al., 2007; Hore et al., 2016), neuroimaging research (Stolp et al., 2018; Zhou et al., 2023), recommendation system analysis (Wang et al., 2019; Zhang et al., 2021), among many others.

This article targets the dependence structures of tensors, and the samples are assumed to follow some tensor normal distributions with a separable covariance matrix. Specifically, we assume that a K -th order tensor $\mathbf{Y} \in \mathbb{R}^{m_1 \times m_2 \times \dots \times m_K} \sim \text{Tnorm}(\mathbf{M}, \Sigma_1 \circ \dots \circ \Sigma_K)$, where “Tnorm” stands for “tensor normal”, \mathbf{M} and $\Sigma_1 \circ \dots \circ \Sigma_K$ respectively represent the tensor mean and covariance, and “ \circ ” is the outer product (Hoff, 2011). Note that, the covariance matrix Σ_k , which is associated with each of the modes, characterizes the *within-mode* dependence structure for $k = 1, \dots, K$, where K is assumed to be fixed. The distribution with such separable covariance structure links to the multivariate normal distribution via $\text{vec}(\mathbf{Y}) \sim \text{mnorm}(\text{vec}(\mathbf{M}), \Sigma_K \otimes \dots \otimes \Sigma_1)$, where $\text{vec}(\cdot)$ denotes the vectorization, $\text{mnorm}(\cdot, \cdot)$ represents a multivariate (vector) normal distribution and \otimes is the Kronecker product. Hence, such a model reduces the ultra-high dimension of the covariance from $\prod_{k=1}^K m_k^2$ to $\sum_{k=1}^K m_k^2$. The verification of the covariance separability is

well studied in the literatures (e.g., Aston et al., 2017; Constantinou et al., 2017; Bagchi and Dette, 2020). In addition, such tensor-normal distribution (with $K \geq 3$) has been widely adopted in many inference problems, see for example, Hoff (2015), Li and Zhang (2017) and Pan et al. (2019). When $K = 2$, it reduces to matrix normal assumption with separable covariance structure, which appears frequently in the literatures as well (Efron, 2009; Leng and Tang, 2012; Zhou, 2014, among others).

1.1 Problem Formulation and Algorithm Sketch

In this article, we focus on the tensor scenarios when $K \geq 3$, and we aim at the alteration detection between mode- k_* dependence structures of the tensor-valued observations from two different groups, where $k_* \in \{1, \dots, K\}$ is a pre-specified mode of interest and the rest of modes are treated as nuisances. Specifically, suppose we observe two groups of independent and identically distributed (i.i.d.) samples: $\{\mathbf{y}_{l,1}\}_{l=1}^{n_1}$ and $\{\mathbf{y}_{l,2}\}_{l=1}^{n_2}$, where

$$\mathbf{y}_{l,d} \in \mathbb{R}^{m_1 \times \dots \times m_K} \stackrel{i.i.d.}{\sim} \text{Tnorm}(\mathbf{M}_d, \Sigma_{1,d} \circ \dots \circ \Sigma_{K,d}), \quad l = 1, \dots, n_d, \quad d = 1, 2. \quad (1.1)$$

In such a model, the covariance matrices are only identifiable up to a constant, namely, $\mathbf{y}_{l,d} \sim \text{Tnorm}(\mathbf{M}_d, (c_{1,d}\Sigma_{1,d}) \circ \dots \circ (c_{K,d}\Sigma_{K,d}))$ holds as long as $\prod_{k=1}^K c_{k,d} = 1$. Hence, instead of covariance and partial covariance, throughout we target the *correlation* matrices $\mathbf{R}_{k_*,d}^{(1)} = \mathbf{D}_{\Sigma_{k_*,d}}^{-1/2} \Sigma_{k_*,d} \mathbf{D}_{\Sigma_{k_*,d}}^{-1/2}$ and the *partial correlation* matrices $\mathbf{R}_{k_*,d}^{(2)} = \mathbf{D}_{\Omega_{k_*,d}}^{-1/2} \Omega_{k_*,d} \mathbf{D}_{\Omega_{k_*,d}}^{-1/2}$, where $\mathbf{D}_{\mathbf{A}}$ is the diagonal matrix of \mathbf{A} and $\Omega_{k_*,d} = \Sigma_{k_*,d}^{-1}$. To unify our analysis, we denote the dependence structures of interest by $\mathbf{P}_{k_*,d} = (\rho_{i,j,d})_{m_{k_*} \times m_{k_*}}$, which can be either $\mathbf{R}_{k_*,d}^{(1)}$ or $\mathbf{R}_{k_*,d}^{(2)}$. Then, one wishes to detect the changes of such dependence structures between the two groups with the control of false discovery. That is, the goal is to test simultaneously

$$H_{0,i,j} : \rho_{i,j,1} = \rho_{i,j,2} \quad \text{v.s.} \quad H_{1,i,j} : \rho_{i,j,1} \neq \rho_{i,j,2}, \quad 1 \leq i < j \leq m_{k_*}, \quad (1.2)$$

with false discovery rate (FDR) and false discovery proportion (FDP) control, and we will carry out the analysis in the following three steps.

The first step is *sample transformation*. It decorrelates and centers the original tensor-valued observations, and then utilizes the nuisance modes to enhance the inference on mode- k_* dependence structure. This step is achieved by plugging in all nuisance covariance matrices and applying a careful orthogonal rotation. Thanks to the separable covariance structure under Model (1.1), by pooling the information from the nuisance modes, the effective sample size increases significantly. This step is crucial for the subsequent analysis and more explanations can be found in Section 2.2.

The second step is *statistic-pair construction*. To be specific, for each $(i, j) \in \mathcal{H} = \{(i, j) : 1 \leq i < j \leq m_{k_*}\}$, a primary t -statistic $T_{i,j}$ is first calculated to quantify the signal strength $\rho_{i,j,1} - \rho_{i,j,2}$. Then, an auxiliary covariate $U_{i,j}$ based on some weighted sum $\rho_{i,j,1} + \kappa_{i,j}\rho_{i,j,2}$ is constructed to capture the sparsity information. Note that, it is often the case that the dependence structure for each group is individually sparse under the high-dimensional setting. Hence, a signal is likely to have a large $|U_{i,j}|$ which differentiates itself from the nulls with $\rho_{i,j,1} = \rho_{i,j,2} = 0$. Therefore, the auxiliary statistic $U_{i,j}$ reflects the heterogeneity of the testing units and can be employed to construct more efficient testing procedures. It is worthwhile to note that, a careful selection of $\kappa_{i,j}$ in the auxiliary statistic is necessary in order to guarantee the validity of the testing algorithm; the details will be provided in Sections 2.3 and 3.1.

As the final step, we propose a novel *Sparsity-Exploited Reranking Algorithm (SERA)*. Instead of directly applying BH procedure (Benjamini and Hochberg, 1995) to the primary sequence $\{T_{i,j}\}$, we employ the earlier constructed auxiliary statistics $\{U_{i,j}\}$ to extract the sparsity knowledge and rerank the p -values. Specifically, a set of locally adaptive weights is constructed based on $\{U_{i,j}\}$ and we place differential weights on each of the p -values obtained through $\{T_{i,j}\}$. Subsequently, the false discovery estimates can

be adjusted and the testing efficiency can be further improved.

1.2 Related Works and Our Contributions

In the literature, there have been a good number of methods proposed to estimate the tensor dependence structures. For example, matrix-valued dependence estimations are studied in Leng and Tang (2012); Yin and Li (2012); Zhou (2014); Zhu and Li (2018); Hornstein et al. (2019); Zhang et al. (2022), among many others, and are further extended to tensor cases, such as tensor covariance estimations (Hoff, 2011; Singull et al., 2012; Manceur and Dutilleul, 2013; Nzabanita et al., 2015) and tensor graphical model estimations (Tsiligkaridis et al., 2013; He et al., 2014; Xu et al., 2017; Min et al., 2022). However, they mostly target one-sample dependence structure recovery and focus on estimation instead of testing, and hence cannot be directly employed to solve our problem (1.2).

The multiple testing problem (1.2) for vector-valued or matrix-valued observations (i.e., $K = 1$ or 2) have been well studied in the literature. Specifically, for vector-valued samples, Xia (2017), Cai and Liu (2016) and Xia et al. (2015) study the simultaneous inference of two-sample covariance/correlation/precision matrices, respectively; for matrix-valued cases, Chen and Liu (2019) targets one-sample precision inference while Chen et al. (2023) and Xia and Li (2019) perform two-sample correlation/partial correlation comparisons respectively; see Table 12 in the supplement of Chen et al. (2023) for a summary of related literatures. When $K \geq 3$, Lyu et al. (2019) considers one-sample inference on the precision matrix of a specific mode but their test cannot be directly extended to the two-sample cases with theoretical guarantees. As will be seen in Section 4.2, a modified two-sample test based on Lyu et al. (2019) often performs poorly.

Our proposal differs from existing solutions and makes several useful contributions. First in terms of problem formulation, to the best of our knowledge, there is no existing

work that solves (1.2) under the current tensor framework. Hence, we fill an important gap in two-sample multiple testing of tensor correlation/partial correlation matrices. To achieve this, we apply a new orthogonal rotation to the tensor-valued observations and take advantage of the separable covariance structures to pool information from the rest $K - 1$ nuisance modes. Through the data pooling, the effective sample size grows from n_d to $n_d \prod_{k \neq k_*} m_k$ which significantly improves the power of the subsequent testing procedure. Second and methodologically, we develop a novel multiple testing method, SERA, for additional testing efficiency improvement. Such power enhancement is approached through the p -value weighting scheme, where the weights are calculated based on a carefully constructed sequence of auxiliary tensor statistics. Besides our tensor dependence testing scenarios, SERA is also generally applicable to many other vector/matrix/tensor two-sample multiple testing problems; see the detailed discussions in Section 3.4. In comparison to the existing multiple testing methods with auxiliary covariates (e.g., Liu, 2014; Cai et al., 2019; Xia et al., 2020), the proposed SERA explores the underlying sparsity structure in a continuous fashion, and enjoys power superiority, dependency robustness and computation efficiency in the meantime; see the detailed explanations and numerical comparisons in Section 4. Hence, our proposal makes a useful addition to the general toolbox of multiple testing with side information. Third and technically, we establish within-mode sample covariance estimation consistency through correlated fibers and derive an overall error bound for the Kronecker product of $K - 1$ nuisance estimates. Moreover, we show the consistency of a Nadaraya-Watson-type kernel estimator (Nadaraya, 1964; Watson, 1964) under a random design, which is to our knowledge not available in the literature. In addition, we extend existing simultaneous error control theories to a new setting with an additional continuous auxiliary sequence, and develop a new set of theoretical tools.

1.3 Organization of the Paper

The rest of the paper is organized as follows. Section 2 studies the implementation of the proposed algorithm. Section 3 collects the theoretical properties. Simulations and real data analysis are provided in Sections 4 and 5 respectively. We relegate some methodological details, all technical proofs, and additional numerical informations to the Online Appendix.

2 Three-Step Inference of T-SERA

This section studies the implementation of the proposed Tensor-valued Sparsity-Exploited Reranking Algorithm, and we name it T-SERA in short. We first introduce some notation and tensor operations in Section 2.1, and then delve into the three-step T-SERA in Sections 2.2 to 2.4.

2.1 Preliminaries

Note that, a K -th order tensor \mathcal{Y} reduces to a vector when $K = 1$ and a matrix when $K = 2$. Denote by $[n] = \{1, 2, \dots, n\}$ for a positive integer n . Then the elements of \mathcal{Y} can be listed as $\{\mathcal{Y}_{i_1, \dots, i_K} : i_k \in [m_k], k \in [K]\}$, with a total number $m = \prod_{k=1}^K m_k$. ‘‘Fibers’’ of a tensor refer to the high-order analogs of matrix rows and columns, and are obtained by fixing all but one of the indices of the tensor (Kolda, 2006). Specifically, any mode- k fiber is a vector of length m_k that is given by $\mathcal{Y}_{i_1, \dots, i_{k-1}, :, i_{k+1}, \dots, i_K}$. For example, a matrix column is a mode-1 fiber and a matrix row is a mode-2 fiber. Hereinafter we denote a mode- k fiber by $\mathcal{Y}_{\{i_j\}_{j \in [K] \setminus k}}$ for $i_j \in [m_j], j \in [K] \setminus k$. Furthermore, we denote the i -th entry of $\mathcal{Y}_{\{i_j\}_{j \in [K] \setminus k}}$ by $\mathcal{Y}_{i, \{i_j\}_{j \in [K] \setminus k}}$, and denote the sub-fiber with the i -th entry removed by $\mathcal{Y}_{-i, \{i_j\}_{j \in [K] \setminus k}}$.

Next, we briefly review the k -mode product of a tensor $\mathcal{Y} \in \mathbb{R}^{m_1 \times m_2 \times \dots \times m_K}$ and a matrix $\mathbf{A} \in \mathbb{R}^{J \times m_k}$ (De Lathauwer et al., 2000). It is denoted by $\mathcal{Y} \times_k \mathbf{A}$, which produces

a new K -th order tensor $\mathcal{V} \in \mathbb{R}^{m_1 \times \dots \times m_{k-1} \times J \times m_{k+1} \times \dots \times m_K}$ with entries

$$\mathcal{V}_{i_1, \dots, i_{k-1}, j, i_{k+1}, \dots, i_K} = \sum_{i_k=1}^{m_k} \mathcal{Y}_{i_1, \dots, i_K} \mathbf{A}_{j, i_k}, \quad j \in [J].$$

Then for a list of matrices $\{\mathbf{A}_1, \dots, \mathbf{A}_K\}$ with $\mathbf{A}_k \in \mathbb{R}^{n_k \times m_k}$ for $k \in [K]$, the Tucker product (Tucker, 1966; Kolda, 2006) of $\mathcal{Y} \in \mathbb{R}^{m_1 \times m_2 \times \dots \times m_K}$ and $\{\mathbf{A}_1, \dots, \mathbf{A}_K\}$ is defined as,

$$\mathcal{Y} \times \{\mathbf{A}_1, \dots, \mathbf{A}_K\} = \mathcal{Y} \times_1 \mathbf{A}_1 \times_2 \mathbf{A}_2 \times \dots \times_K \mathbf{A}_K,$$

which yields a $n_1 \times \dots \times n_K$ tensor.

2.2 Step 1: Sample Transformation

We first explain the transformation idea for the oracle case where all nuisance covariance matrices are known. Then we provide a fully data-driven implementation in Algorithm 1.

For $d = 1, 2$, we first stack n_d observed tensors into a $(K + 1)$ -th order tensor denoted by $\mathcal{Y}_d = (\mathcal{Y}_{1,d}, \dots, \mathcal{Y}_{n_d,d})$. It is easy to check that $\mathcal{Y}_d \sim \text{Tnorm}(\mathcal{M}_d \circ \mathbf{1}_{n_d}, \boldsymbol{\Sigma}_{1,d} \circ \dots \circ \boldsymbol{\Sigma}_{K,d} \circ \mathbf{I}_{n_d})$ by Proposition 3 in the Online Appendix, where $\mathbf{1}_{n_d} \in \mathbb{R}^{n_d}$ is a vector repeating 1's and $\mathbf{I}_{n_d} \in \mathbb{R}^{n_d \times n_d}$ is an identity matrix. The proposed transformation has two goals: *decorrelation* and *centralization*, and can be achieved in a one-step operation. Decorrelation aims to make all mode- k_* fibers independent and have identical covariance matrices; it can be accomplished by plugging in all true nuisance covariance matrices. For centralization, we rotate the tensor-valued observations by any orthogonal matrices $\{\mathbf{Q}_d \in \mathbb{R}^{n_d \times n_d} : d = 1, 2\}$ with the last row equal to $(1/\sqrt{n_d}, \dots, 1/\sqrt{n_d})$; it transfers the means $\{\mathcal{M}_d : d = 1, 2\}$ to zero tensors. Specifically, we transform the original samples by the following Tucker product:

$$\mathcal{Z}_d^o = \mathcal{Y}_d \times \{\boldsymbol{\Sigma}_{1,d}^{-1/2}, \dots, \boldsymbol{\Sigma}_{k_*-1,d}^{-1/2}, \mathbf{I}_{m_{k_*}}, \boldsymbol{\Sigma}_{k_*+1,d}^{-1/2}, \dots, \boldsymbol{\Sigma}_{K,d}^{-1/2}, \mathbf{Q}_d\}.$$

Then by the propositions in Section S1.1 of the Online Appendix, we obtain that,

$$(\mathcal{Z}_{1,d}^o, \dots, \mathcal{Z}_{n_d-1,d}^o) \sim \text{Tnorm}(\mathbf{0}, \mathbf{I}_{m_1} \circ \dots \circ \mathbf{I}_{m_{k_*-1}} \circ \Sigma_{k_*,d} \circ \mathbf{I}_{m_{k_*+1}} \dots \circ \mathbf{I}_{m_K} \circ \mathbf{I}_{n_d-1}), \quad (2.1)$$

which enables us to pool all i.i.d. mode- k_* fibers of $\{(\mathcal{Z}_{1,d}^o, \dots, \mathcal{Z}_{n_d-1,d}^o) : d = 1, 2\}$ for the subsequent inference.

However, the nuisances are usually unknown in practice, and we thus turn to their consistent estimates. Specifically, for $k \in [K] \setminus k_*$, $d = 1, 2$, let $\hat{\Sigma}_{k,d}$ be some consistent estimate of $\Sigma_{k,d}$, and we can transform the samples by

$$\mathcal{Z}_d = \mathcal{Y}_d \times \left\{ \hat{\Sigma}_{1,d}^{-1/2}, \dots, \hat{\Sigma}_{k_*-1,d}^{-1/2}, \mathbf{I}_{m_{k_*}}, \hat{\Sigma}_{k_*+1,d}^{-1/2}, \dots, \hat{\Sigma}_{K,d}^{-1/2}, \mathbf{Q}_d \right\}.$$

Then all mode- k_* fibers of $(\mathcal{Z}_{1,d}, \dots, \mathcal{Z}_{n_d-1,d})$ can be seen as nearly i.i.d. observations if the covariances are appropriately estimated, and hence can be pooled to assist the inference. We summarize the above transformations in Algorithm 1.

Remark 1. *First, the original sample size n_d should be larger than one for a proper sample transformation according to Equation (2.1). Second, though the covariance of each mode is only identifiable up to a constant, such non-identifiability will not affect the test due to the standardization step in the following statistics construction; see more details in Section S2 of the Online Appendix. Third, for each $k \neq k_*$, all mode- k fibers can be pooled to estimate the corresponding nuisance covariance, and therefore consistent nuisance estimations described in the first step of Algorithm 1 are easily attainable; see examples in Remark 3 of Section 3.1. One can also directly pool correlated fibers in the original samples \mathcal{Y}_d to estimate the dependence structure of interest, it nevertheless introduces a non-negligible bias in the following variance estimations in quantifying test heterogeneities. As shown later in Section 4, the proposed data-driven algorithm indeed well emulates the oracle case with known nuisances and it outperforms the competing methods without such sample transformation.*

Algorithm 1 (Step 1) Sample transformation.

Input: Original samples $\{(\mathbf{y}_{1,d}, \dots, \mathbf{y}_{n_d,d}) : d = 1, 2\}$.

1. **Nuisance estimation:** Obtain $\{\hat{\Sigma}_{k,d} : k \in [K] \setminus k_*, d = 1, 2\}$ that satisfy Condition (A2) in Section 3.1.
2. **Orthogonalization:** Generate orthogonal matrices $\{\mathbf{Q}_d \in \mathbb{R}^{n_d \times n_d} : d = 1, 2\}$, with the last row equal to $(1/\sqrt{n_d}, \dots, 1/\sqrt{n_d})$.
3. **Decorrelation and Centralization:** For $l \in [n_d], d = 1, 2$, calculate

$$\mathbf{z}_{l,d} = \mathbf{y}_{l,d} \times \left\{ \hat{\Sigma}_{1,d}^{-1/2}, \dots, \hat{\Sigma}_{k_*-1,d}^{-1/2}, \mathbf{I}_{m_{k_*}}, \hat{\Sigma}_{k_*+1,d}^{-1/2}, \dots, \hat{\Sigma}_{K,d}^{-1/2}, \mathbf{Q}_d \right\}.$$

Output: Transformed samples $\{(\mathbf{z}_{1,d}, \dots, \mathbf{z}_{n_d-1,d}) : d = 1, 2\}$.

2.3 Step 2: Statistic Pairs Construction

Based on the transformed samples $\{(\mathbf{z}_{1,d}, \dots, \mathbf{z}_{n_d-1,d}) : d = 1, 2\}$, we next construct the statistic pairs $\{(T_{i,j}, U_{i,j}) : (i, j) \in \mathcal{H}\}$ in this section.

Recall that we focus on the comparison of the dependence structures $\{\mathbf{P}_{k_*,d}, d = 1, 2\}$ for a specific mode k_* . We will consider two scenarios in turn, first $\mathbf{P}_{k_*,d} = \mathbf{R}_{k_*,d}^{(1)}$ (hereinafter the correlation scenario) and then $\mathbf{P}_{k_*,d} = \mathbf{R}_{k_*,d}^{(2)}$ (hereinafter the partial correlation scenario).

Under both scenarios, we will construct a set of primary t -statistics as well as an auxiliary sequence that captures the sparsity information. Specifically, based on the transformed samples output by Algorithm 1, we estimate the correlation and partial correlation coefficients by $\hat{\rho}_{i,j,d}$'s (i.e., Equation (2.3) in Algorithm 2 and Equation (2.5) in Algorithm 3), whose variances will be further approximated by $\hat{\nu}_{i,j,d}$'s to handle the heterogeneity (i.e., Equation (2.4) in Algorithm 2 and Equation (2.6) in Algorithm 3). Then based on these estimates, we construct a pair of statistics $(T_{i,j}, U_{i,j})$ for each single

hypothesis:

$$T_{i,j} = \frac{\hat{\rho}_{i,j,1} - \hat{\rho}_{i,j,2}}{(\hat{\nu}_{i,j,1} + \hat{\nu}_{i,j,2})^{1/2}}, \quad U_{i,j} = \frac{\hat{\rho}_{i,j,1} + \hat{\kappa}_{i,j}\hat{\rho}_{i,j,2}}{(\hat{\nu}_{i,j,1} + \hat{\kappa}_{i,j}^2\hat{\nu}_{i,j,2})^{1/2}}, \quad (i, j) \in \mathcal{H}, \quad (2.2)$$

where $\hat{\kappa}_{i,j} = \hat{\nu}_{i,j,1}/\hat{\nu}_{i,j,2}$. The detailed constructions are provided in Algorithm 2 (the correlation scenario) and Algorithm 3 (the partial correlation scenario); more insights on the estimations in each of these two algorithms are collected in Section S2 of the Online Appendix. It is important to note that, the primary sequence $\{T_{i,j}\}$ in (2.2) collects t -statistics that quantify the signal strengths of the multiple testing problem (1.2), while the auxiliary sequence $\{U_{i,j}\}$ in (2.2) reflects the sparsity heterogeneity of the testing units and hence can be employed to adjust and rerank the p -values obtained through the primary statistics in order to improve the testing efficiency; this will be explained further in Section 2.4. In addition, the construction in (2.2) guarantees the asymptotic independence between the two sequences (as will be shown in Theorem 1 below), which is essential for the subsequent testing validity analysis.

Remark 2. *A few remarks are collected. The estimation step (2.3) in Algorithm 2 is flexible and it is not restricted to the sample correlation approach provided here. Other consistent correlation estimations that satisfy certain convergence rate can be employed as well (e.g., Cai and Liu, 2016). In comparison, for partial correlation case in Algorithm 3, due to the bias introduced by node-wise regression, the two-sample inference of the partial correlation matrices is much more involved. We extend the ideas proposed in Xia et al. (2015); Xia and Li (2019) to estimate the partial correlations. Though there exist some other partial correlation inference methods (e.g., Chen and Liu, 2019; Lyu et al., 2019), they all target one-sample inference and cannot directly deal with two-sample cases. Nevertheless, we extend their work to the two-sample scenarios in Section 4 (without theoretical guarantee) and our method presents superior performance in terms of both FDR control and power compared to theirs. The detailed description of such*

Algorithm 2 (Step 2 for correlation scenario) Statistic pairs construction.

Input: Transformed samples $\{(\mathbf{Z}_{1,d}, \dots, \mathbf{Z}_{n_d-1,d}) : d = 1, 2\}$ from Algorithm 1.

1. **Estimate correlation:** Estimate the mode- k_* correlation matrices by

$$\hat{\rho}_{i,j,d} = \frac{\hat{\sigma}_{i,j,d}}{(\hat{\sigma}_{i,i,d}\hat{\sigma}_{j,j,d})^{1/2}}, 1 \leq i \leq j \leq m_{k_*}, d = 1, 2, \quad (2.3)$$

where

$$(\hat{\sigma}_{i,j,d}) = \frac{m_{k_*}}{(n_d - 1)m} \sum_{l=1}^{n_d-1} \sum_{i_k=1, k \in [K] \setminus k_*}^{m_k} \mathbf{Z}_{\{i_k\}_{k \in [K] \setminus k_*}, l, d} \mathbf{Z}_{\{i_k\}_{k \in [K] \setminus k_*}, l, d}^\top.$$

2. **Quantify heterogeneity:** Estimate the variance of $\hat{\rho}_{i,j,d}$ by

$$\hat{\nu}_{i,j,d} = \frac{\sum_{l=1}^{n_d-1} \sum_{i_k=1, k \in [K] \setminus k_*}^{m_k} \left(\mathbf{Z}_{i, \{i_k\}_{k \in [K] \setminus k_*}, l, d} \mathbf{Z}_{j, \{i_k\}_{k \in [K] \setminus k_*}, l, d} - \hat{\sigma}_{i,j,d} \right)^2}{\{(n_d - 1)m/m_{k_*}\}^2 \hat{\sigma}_{i,i,d} \hat{\sigma}_{j,j,d}}. \quad (2.4)$$

Output: Collection of statistic pairs $\{(T_{i,j}, U_{i,j}) : (i, j) \in \mathcal{H}\}$ via Equation (2.2).

extension is provided in Section S5 of the Online Appendix. Finally, Condition (A3') for the node-wise regression estimates can be easily satisfied and will be discussed further in Remark 3.

2.4 Step 3: A Power Enhanced Procedure SERA

We propose in this section the procedure SERA that further improves the power of the test. Note that, SERA can be generally applied to any two-sample large-scale inference problems with sparsity structure and is not restricted to our tensor setting. Hence it is of independent interest and will be discussed further in Section 3.4. We now describe the main idea of SERA and the details will be summarized in Algorithm 4. To be specific, we first introduce and estimate a sparsity level, and then obtain a sequence of weighted p -values. Finally, we approximate and control the FDP.

Algorithm 3 (Step 2 for partial correlation scenario) Statistic pairs construction.

Input: Transformed samples $\{(\mathbf{Z}_{1,d}, \dots, \mathbf{Z}_{n_d-1,d}) : d = 1, 2\}$ from Algorithm 1.

1. **Estimate partial covariance:** Obtain regression coefficient estimates $\{\hat{\boldsymbol{\eta}}_{i,d}\}$ that satisfy Condition (A3') in Section 3.1, and calculate residuals $\hat{\xi}_{i,\{i_k\}_{k \in [K] \setminus k_*},l,d} = \mathbf{Z}_{i,\{i_k\}_{k \in [K] \setminus k_*},l,d} - \mathbf{Z}_{-i,\{i_k\}_{k \in [K] \setminus k_*},l,d}^\top \hat{\boldsymbol{\eta}}_{i,d}$, $i \in [m_{k_*}]$, $d = 1, 2$. Calculate sample covariance of residuals:

$$\tilde{r}_{i,j,d} = \frac{m_{k_*}}{(n_d - 1)m} \sum_{l=1}^{n_d-1} \sum_{i_k=1, k \in [K] \setminus k_*}^{m_k} \left(\hat{\xi}_{i,\{i_k\}_{k \in [K] \setminus k_*},l,d} \hat{\xi}_{j,\{i_k\}_{k \in [K] \setminus k_*},l,d} \right).$$

2. **Debiasing:** Debias $\tilde{r}_{i,j,d}$ by

$$\begin{aligned} \hat{r}_{i,j,d} &= -(\tilde{r}_{i,j,d} + \tilde{r}_{i,i,d} \hat{\eta}_{i,j,d} + \tilde{r}_{j,j,d} \hat{\eta}_{j-1,i,d}), \quad (i, j) \in \mathcal{H}, \\ \hat{r}_{i,i,d} &= \tilde{r}_{i,i,d}, \quad i \in [m_{k_*}]. \end{aligned}$$

3. **Estimate partial correlation:** Calculate

$$\hat{\rho}_{i,j,d} = \frac{\hat{r}_{i,j,d}}{(\hat{r}_{i,i,d} \hat{r}_{j,j,d})^{1/2}}, \quad (i, j) \in \mathcal{H}, d = 1, 2. \quad (2.5)$$

4. **Quantify heterogeneity:** Estimate the variance of $\hat{\rho}_{i,j,d}$ by

$$\hat{\nu}_{i,j,d} = (1 + \hat{\eta}_{i,j,d}^2 \hat{r}_{i,i,d} / \hat{r}_{j,j,d}) / \{(n_d - 1)m / m_{k_*}\}. \quad (2.6)$$

Output: Collection of statistic pairs $\{(T_{i,j}, U_{i,j}) : (i, j) \in \mathcal{H}\}$ via Equation (2.2).

Recall that, the auxiliary sequence reflects the sparsity heterogeneity among the tests. Hence, we incorporate such sequence and define a *posterior local sparsity level* providing the auxiliary variable $U_{i,j}$ by

$$\pi(U_{i,j}) = \Pr(\theta_{i,j} = 1 | U_{i,j}),$$

where $\theta_{i,j} = \mathbb{I}(\rho_{i,j,1} \neq \rho_{i,j,2})$ for each hypothesis and $\mathbb{I}(\cdot)$ is an indicator function. This sparsity level reflects the chance of signal occurrence and the goal of SERA is to use such

quantity to adjust the significance of the tests. Since $\pi(U_{i,j})$ is unknown, the first step of SERA estimates $\pi(U_{i,j})$ by $\hat{\pi}^\tau(U_{i,j})$ using a kernel-based approach following similar ideas in Cai et al. (2022) and Ma et al. (2023), where τ is a pre-specified screening parameter; see Equation (2.8) in Algorithm 4.

Next, we calculate the p -values by the asymptotic normality result of the primary sequence $\{T_{i,j}\}$ (Theorem 1 in Section 3.1), and construct a set of locally adaptive weights based on the auxiliary sequence $\{U_{i,j}\}$. We employ the weighting scheme proposed in Cai et al. (2022); Ma et al. (2023), namely, the weights $\hat{w}(U_{i,j}) = \hat{\pi}^\tau(U_{i,j})/\{1 - \hat{\pi}^\tau(U_{i,j})\}$ are placed on each of the p -values and the adjusted p -values are obtained by $\{p_{i,j}^{\hat{w}} = p_{i,j}/\hat{w}(U_{i,j}) : (i,j) \in \mathcal{H}\}$. Intuitively, a larger $\pi(U_{i,j})$ indicates a higher chance of signal occurrence and leads to a smaller weighted p -value, and hence yields a higher rejection possibility for the hypothesis with index (i,j) . Such weighting scheme provides a better ranking of the tests by incorporating the sparsity information from the auxiliary sequence. It is worth noting that, the weighting approach in Step 2(a) of Algorithm 4 can be flexible. Besides the approach provided here, one can employ other methods as well (e.g., Li and Barber, 2019; Liang et al., 2023).

Finally, we select a cutoff for the weighted p -values so that the estimated FDP does not exceed a pre-specified significance level $\alpha \in (0, 1)$. Denote by $\delta_{i,j}^{\text{T-SERA}}(t) = \mathbb{I}(p_{i,j}^{\hat{w}} \leq t)$ the decision rule of T-SERA for the (i,j) -th hypothesis with threshold t ; $\delta_{i,j}^{\text{T-SERA}}(t) = 1$ if we reject the null and $\delta_{i,j}^{\text{T-SERA}}(t) = 0$ otherwise. Then,

$$\text{FDP}\{\boldsymbol{\delta}^{\text{T-SERA}}(t)\} = \frac{\sum_{(i,j) \in \mathcal{H}} [\{1 - \theta_{i,j}\} \delta_{i,j}^{\text{T-SERA}}(t)]}{\max\left\{\sum_{(i,j) \in \mathcal{H}} \delta_{i,j}^{\text{T-SERA}}(t), 1\right\}}, \quad \text{FDR}^{\text{T-SERA}} = \mathbf{E}[\text{FDP}\{\boldsymbol{\delta}^{\text{T-SERA}}(t)\}], \quad (2.7)$$

where $\boldsymbol{\delta}^{\text{T-SERA}}(t) = \{\delta_{i,j}^{\text{T-SERA}}(t) : (i,j) \in \mathcal{H}\}$ collects all decision rules under the threshold t . To estimate and control FDP, note that the denominator of FDP is known and the numerator can be estimated by approximating its expectation. More precisely, with known $\pi(U_{i,j})$'s and a given threshold t , the expected number of false rejections equals

Algorithm 4 (Step 3) The power enhanced procedure SERA.

Input: (a) Statistic pairs $\{(T_{i,j}, U_{i,j}) : (i, j) \in \mathcal{H}\}$ from Algorithm 2 or 3;
 (b) Kernel function $\mathbb{K}(\cdot)$ and bandwidth h ;
 (c) Screen threshold τ and significance level α .

1. Posterior Sparsity Level Estimation:

- (a) Calculate the p -values: $p_{i,j} = 2\{1 - \Phi(|T_{i,j}|)\}$, $(i, j) \in \mathcal{H}$, where $\Phi(\cdot)$ is the cumulative distribution function (CDF) of a standard normal variable;
- (b) Determine the screen set: $\mathcal{I}(\tau) = \{(i', j') \in \mathcal{H} : p_{i',j'} > \tau\}$;
- (c) Kernel estimation:

$$\hat{\pi}^\tau(U_{i,j}) = 1 - \frac{\sum_{(i',j') \in \mathcal{I}(\tau)} v_h(U_{i,j}, U_{i',j'})}{(1 - \tau) \sum_{(i',j') \in \mathcal{H}} v_h(U_{i,j}, U_{i',j'})}, \quad (2.8)$$

$$\text{where } v_h(U_{i,j}, U_{i',j'}) = \frac{\mathbb{K}_h(U_{i,j} - U_{i',j'})}{\mathbb{K}_h(0)}, \mathbb{K}_h(x) = 1/h\mathbb{K}(x/h).$$

2. Reranking and Thresholding:

- (a) Weigh p -values by $p_{i,j}^{\hat{w}} = p_{i,j}/\hat{w}(U_{i,j})$, where $\hat{w}(U_{i,j}) = \frac{\hat{\pi}^\tau(U_{i,j})}{1 - \hat{\pi}^\tau(U_{i,j})}$, $(i, j) \in \mathcal{H}$;
- (b) Rank the weighted p -values in ascending order: $p_{(1)}^{\hat{w}}, \dots, p_{(|\mathcal{H}|)}^{\hat{w}}$, where $|\mathcal{H}|$ is the cardinality of \mathcal{H} ;
- (c) Search for $\hat{q} = \max \left\{ q \in [|\mathcal{H}|] : q^{-1} \sum_{(i,j) \in \mathcal{H}} \hat{\pi}(U_{i,j}) p_{(q)}^{\hat{w}} \leq \alpha \right\}$;
- (d) Determine the decision $\delta_{i,j}^{\text{T-SERA}}(p_{(\hat{q})}^{\hat{w}}) = \mathbb{I}(p_{i,j}^{\hat{w}} \leq p_{(\hat{q})}^{\hat{w}})$ for each $(i, j) \in \mathcal{H}$.

Output: Collection of decisions $\delta^{\text{T-SERA}}(p_{(\hat{q})}^{\hat{w}}) = \{\delta_{i,j}^{\text{T-SERA}}(p_{(\hat{q})}^{\hat{w}}) : (i, j) \in \mathcal{H}\}$.

to $\mathbb{E} \left[\sum_{(i,j) \in \mathcal{H}} \Pr \{ \theta_{i,j} = 0, \delta_{i,j}^{\text{T-SERA}}(t) = 1 | U_{i,j} \} \right] \approx \mathbb{E} \left\{ \sum_{(i,j) \in \mathcal{H}} \pi(U_{i,j}) t \right\}$, where the approximation comes from the asymptotic independence between $T_{i,j}$ and $U_{i,j}$ as shown in Theorem 1. Hence, the number of false rejections, i.e., the numerator of FDP, can be estimated by $\sum_{(i,j) \in \mathcal{H}} \hat{\pi}^\tau(U_{i,j}) t$. The above steps are summarized in Algorithm 4.

3 Theoretical Properties

To better interpret the procedures in the previous section, we study in Section 3.1 the asymptotic properties of the statistic pairs (2.2) including the asymptotic normality and independence results. Next, the error rates control of the proposed T-SERA will be explored in Section 3.3 and it starts with the estimation consistency result of the posterior local sparsity level in Section 3.2.

We begin with some notation. For two sequences of real numbers $\{a_n\}$ and $\{b_n\}$: write $a_n = O(b_n)$ if there exists a constant C such that $|a_n| \leq C|b_n|$ for any sufficiently large n ; write $a_n \asymp b_n$ if there exists constants $0 < c < C$ such that $c|b_n| \leq |a_n| \leq C|b_n|$ for any sufficiently large n ; and write $a_n = o(b_n)$ if $\lim_{n \rightarrow \infty} a_n/b_n = 0$. For a matrix \mathbf{A} , denote by $\lambda_g(\mathbf{A})$ the g -th largest eigenvalue of \mathbf{A} . Let $n = n_1 + n_2$ and $\tilde{m} = \max(\{m_k\}_{k \neq k_*})$. For $l \in [n_d - 1]$, denote by $\text{Cov}^{-1}(\mathcal{Z}_{\{i_k\}_{k \in [K] \setminus k_*}, l, d}) = (\tilde{\omega}_{i,j,d}^l)$ and $s_0 = \max_{i,l,d} \sum_{j=1}^{m_{k_*}} \max\{\mathbb{I}(\tilde{\omega}_{i,j,d}^l \neq 0), \mathbb{I}(\omega_{i,j,d} \neq 0)\}$; let $\boldsymbol{\eta}_{i, \{i_k\}_{k \in [K] \setminus k_*}, d}$ be the true coefficient by regressing $\mathcal{Z}_{i, \{i_k\}_{k \in [K] \setminus k_*}, l, d}$ on $\mathcal{Z}_{-i, \{i_k\}_{k \in [K] \setminus k_*}, l, d}$.

3.1 Asymptotic Normality and Independence of Statistic Pairs

This section first collects some regularity conditions, and then establishes the asymptotic normalities and asymptotic independence of $T_{i,j}$ and $U_{i,j}$ defined in Equation (2.2).

(A1) Suppose $n_1 \asymp n_2$, $n_d \geq 2$, and for any $k \in [K]$, $\lambda_1(\boldsymbol{\Sigma}_{k,d}) \asymp \lambda_{m_k}(\boldsymbol{\Sigma}_{k,d}) \asymp 1$, $d = 1, 2$.

(A2) Assume that uniformly in $k \in [K] \setminus k_*$, for some constant $C_1 > 5$, there exist some constants $C_0, c_{k,d} > 0$ such that

$$\Pr \left\{ \left\| \hat{\boldsymbol{\Sigma}}_{k,d} - c_{k,d} \boldsymbol{\Sigma}_{k,d} \right\|_{\infty} \geq C_0 \left\{ \log m_k / (n_d m / m_k) \right\}^{1/2} \right\} = O(m_{k_*}^{-C_1}).$$

(A3) Suppose $\log m_{k_*} = o\{(nm/m_{k_*})^{1/5}\}$ and $\tilde{m}^3 \log \tilde{m} \log m_{k_*} \log^2 \max(\tilde{m}, m_{k_*}, n) = o(nm_{k_*})$.

(A3') Suppose $\log m_{k_*} = o\{(nm/m_{k_*})^{1/5}\}$, $s_0^2 \tilde{m}^3 \log \tilde{m} \log^3 \max(\tilde{m}, m_{k_*}, n) = o(nm_{k_*})$, and $\{s_0 \tilde{m}^3 \log \tilde{m} \log \max(\tilde{m}, m_{k_*}, n)\}^2 m \log m_{k_*} = o(nm_{k_*}^3)$. Suppose $\{\hat{\boldsymbol{\eta}}_{i,d}\}$ satisfy that

$$\Pr \left\{ \max_{i \in [m_{k_*}], \{i_k \in [m_k]\}_{k \in [K] \setminus k_*}} |\hat{\boldsymbol{\eta}}_{i,d} - \boldsymbol{\eta}_{i, \{i_k\}_{k \in [K] \setminus k_*}, d}|_1 \geq a_{m1} \right\} = O(m_{k_*}^{-C_1}),$$

$$\Pr \left\{ \max_{i \in [m_{k_*}], \{i_k \in [m_k]\}_{k \in [K] \setminus k_*}} |\hat{\boldsymbol{\eta}}_{i,d} - \boldsymbol{\eta}_{i, \{i_k\}_{k \in [K] \setminus k_*}, d}|_2 \geq a_{m2} \right\} = O(m_{k_*}^{-C_1}),$$

where $a_{m1} = o(\{\log \max(m_{k_*}, \tilde{m}, n)\}^{-1})$, $a_{m2} = o(\{(nm/m_{k_*}) \log m_{k_*}\}^{-1/4})$.

Remark 3. Condition (A1) states some covariance regularity conditions that are commonly assumed in the high-dimensional inference literatures on vector/matrix/tensor covariance/precision matrices (e.g., Bickel and Levina, 2008; Leng and Tang, 2012; Chen and Liu, 2019; Lyu et al., 2019). We assume $n_d \geq 2, d = 1, 2$ for a proper sample transformation as explained in Remark 1. It is not required if the original samples are centered (as assumed in, e.g., Xia and Li, 2017, 2019; Lyu et al., 2019). Condition (A2) poses some rate requirements on the nuisance covariance estimates, which can be easily satisfied by, e.g., sample covariance estimator, the banded estimator (Bickel and Levina, 2008) or adaptive thresholding estimator (Cai and Liu, 2011), under some mild conditions. Note that, the test statistics in (2.2) are not affected by any deterministic constants $\{c_{k,d} : k \in [K] \setminus k_*, d = 1, 2\}$ as discussed in Remark 1. Alternatively, one can also employ any precision estimates satisfying $\Pr\{\|\hat{\boldsymbol{\Omega}}_{k,d} - c_{k,d}^{-1} \boldsymbol{\Omega}_{k,d}\|_2 \geq Cm_k \{\log m_k / (n_d m / m_k)\}^{1/2}\} = O(m_{k_*}^{-C_1})$ and the sample transformation in Algorithm 1 can be performed by $\mathbf{Z}_d = \mathbf{Y}_d \times \{\hat{\boldsymbol{\Omega}}_{1,d}^{1/2}, \dots, \hat{\boldsymbol{\Omega}}_{k_*-1,d}^{1/2}, \mathbf{I}_{m_{k_*}}, \hat{\boldsymbol{\Omega}}_{k_*+1,d}^{1/2}, \dots, \hat{\boldsymbol{\Omega}}_{K,d}^{1/2}, \mathbf{Q}_d\}$ instead. Conditions (A3) and (A3') assume some relationships between the sample size and the tensor dimensionalities and are similar to or milder than those in the matrix scenarios (Chen et al., 2023; Xia and Li, 2017, 2019). Both conditions can be further relaxed if some additional covariance sparsity assumptions are imposed. Condition (A3') also

regularizes the regression coefficient estimates that can be obtained via Dantzig selector, Lasso, etc., under some mild conditions.

Let $\mathcal{H}_0 = \{(i, j) \in \mathcal{H} : \theta_{i,j} = 0\}$ and $G(t) = 2\{1 - \Phi(t)\}$. Denote by $\hat{\rho}_{i,j,d}^o$ the oracle counterpart of $\hat{\rho}_{i,j,d}$ that is derived from the oracle transformed samples $\{\mathbf{Z}_{l,d}^o\}_{l=1}^{n_d-1}$ in (2.1), and denote by $\nu_{i,j,d}$ the theoretical variance of $\hat{\rho}_{i,j,d}^o$; the detailed expressions are provided in Section S2 of the Online Appendix. Then, we have the following results.

Theorem 1. *Suppose Conditions (A1), (A2) and (A3) hold if $\mathbf{P}_{k^*,d} = \mathbf{R}_{k^*,d}^{(1)}$, or Conditions (A1), (A2) and (A3') hold if $\mathbf{P}_{k^*,d} = \mathbf{R}_{k^*,d}^{(2)}$. Let $\rho_{i,j,1} = \rho_{i,j,2} = \rho_{i,j}$ under the null. Then,*

$$\begin{aligned} \Pr \left\{ \max_{(i,j) \in \mathcal{H}_0} \left| T_{i,j} - b_{i,j} - \frac{\hat{\rho}_{i,j,1}^o - \hat{\rho}_{i,j,2}^o}{(\nu_{i,j,1} + \nu_{i,j,2})^{1/2}} \right| \geq e_m \right\} &= O(m_{k^*}^{-C_1}), \\ \Pr \left\{ \max_{(i,j) \in \mathcal{H}_0} \left| U_{i,j} - b_{i,j} - \mu_{i,j} - \frac{\hat{\rho}_{i,j,1}^o - \rho_{i,j,1} + \kappa_{i,j}(\hat{\rho}_{i,j,2}^o - \rho_{i,j,2})}{(\nu_{i,j,1} + \kappa_{i,j}^2 \nu_{i,j,2})^{1/2}} \right| \geq e_m \right\} &= O(m_{k^*}^{-C_1}), \end{aligned} \quad (3.1)$$

where $\kappa_{i,j} = \nu_{i,j,1}/\nu_{i,j,2}$, $e_m = o\{(\log m_{k^*})^{-1/2}\}$, $\mu_{i,j} = (1 + e_m^2) \frac{\rho_{i,j,1} + \kappa_{i,j} \rho_{i,j,2}}{(\nu_{i,j,1} + \kappa_{i,j}^2 \nu_{i,j,2})^{1/2}}$, and $b_{i,j} = O\{(\log m_{k^*})^{1/2} \rho_{i,j}\}$ and satisfies $\Pr \{ \max_{(i,j) \in \mathcal{S}} |b_{i,j}| \geq x \} \leq O(|\mathcal{S}| \{1 - \Phi(x)\} + m_{k^*}^{-1})$ uniformly in $(\log m_{k^*})^{1/4} \leq x \leq (8 \log m_{k^*})^{1/2}$ and $\mathcal{S} \subset \mathcal{H}$. In addition, for some constant $C_2 > 2$,

$$\Pr_{(i,j) \in \mathcal{H}_0} \{ |T_{i,j} - b_{i,j}| \geq t | U_{i,j} \} = \{1 + o(1)\} G(t) + O(m_{k^*}^{-C_2}), \quad (3.2)$$

uniformly in $|t| = O\{(\log m_{k^*})^{1/2}\}$, $|U_{i,j} - b_{i,j} - \mu_{i,j}| = O\{(\log m_{k^*})^{1/2}\}$ and all $(i, j) \in \mathcal{H}_0$.

Theorem 1 states the asymptotic normality of both $T_{i,j}$ and $U_{i,j}$, and also the asymptotic independence between them. The normality results enable us to derive the null distribution of the test statistics and handle the dependence among the hypotheses. The asymptotic independence is essential to SERA, because it ensures that the null distribution of the primary sequence is not distorted by incorporating the auxiliary covariates

into the inference. Finally, the term $b_{i,j}$ introduces an additional bias for the two-sample setting, because $\rho_{i,j,d}$'s are not necessarily equal to zero under the null. It adds difficulties in extending the existing asymptotic normality results in the one-sample literatures (e.g., Chen and Liu, 2019; Lyu et al., 2019) as well as in handling the dependence structures for the subsequent FDR analysis.

3.2 Estimation Consistency of the Posterior Sparsity Level

Next, we show the consistency of $\hat{\pi}^\tau(U_{i,j})$ in Equation (2.8) to its theoretical counterpart

$$\pi^\tau(U_{i,j}) = 1 - \frac{\Pr\{p_{i,j} > \tau | U_{i,j}\}}{1 - \tau}, \quad (3.3)$$

which is a conservative approximation of $\pi(U_{i,j})$. We consider such an intermediate quantity (3.3) because a direct estimation of $\pi(U_{i,j})$ is difficult; see the explanations in Cai et al. (2022) and Ma et al. (2023).

Denote by $f_{i',j'}(\cdot | U_{i,j})$ the conditional density function of $U_{i',j'}$ given $U_{i,j}$ and \mathbf{H} the Hessian matrix of $\Pr(p_{i',j'} > \tau | U_{i',j'}, U_{i,j})$. We first introduce some regularity conditions.

(A4) Suppose the kernel function $\mathbb{K}(x) : \mathbb{R} \rightarrow \mathbb{R}$ is positive, unimodal and satisfies

$$\int_{\mathbb{R}} \mathbb{K}(x) = 1, \int_{\mathbb{R}} x \mathbb{K}(x) = 0, \text{ and } \int_{\mathbb{R}} x^2 \mathbb{K}(x) < \infty.$$

(A5) Let $\Lambda_{i,j} = \{U_{i,j} : \text{with probability } 1 - O(m_{k_*}^{-2}), \text{ uniformly for all } (i', j') \in \mathcal{H}, f_{i',j'}(\cdot | U_{i,j}) \text{ is bounded, } \Pr(p_{i',j'} > \tau | U_{i',j'}, U_{i,j}) \text{ has continuous first and second partial derivatives at } (U_{i',j'}, U_{i,j})^\top, \text{ and } \lambda_g(\mathbf{H}) = O(1) \text{ for } g = 1, 2\}$. Suppose $\Pr(\Lambda_{i,j}) \rightarrow 1$ uniformly for all $(i, j) \in \mathcal{H}$ as $m_{k_*} \rightarrow \infty$.

(A6) Suppose uniformly for all $(i, j) \in \mathcal{H}$, as $m_{k_*} \rightarrow \infty$, with probability tending to 1,

$$\begin{aligned} & \text{Var} \left(\sum_{(i', j') \in \mathcal{H}} [\mathbb{K}_h(U_{i,j} - U_{i', j'}) \mathbb{I}(p_{i,j} > \tau)] | U_{i,j} \right) \\ &= O \left(\sum_{(i', j') \in \mathcal{H}} \text{Var} [\mathbb{K}_h(U_{i,j} - U_{i', j'}) \mathbb{I}(p_{i,j} > \tau) | U_{i,j}] \right), \end{aligned}$$

and

$$\text{Var} \left(\sum_{(i', j') \in \mathcal{H}} \mathbb{K}_h(U_{i,j} - U_{i', j'}) | U_{i,j} \right) = O \left(\sum_{(i', j') \in \mathcal{H}} \text{Var} [\mathbb{K}_h(U_{i,j} - U_{i', j'}) | U_{i,j}] \right).$$

Condition (A4) holds naturally for the commonly used kernels, and Condition (A5) regulates the first and second derivatives of the conditional CDFs and is mild too. Condition (A6) can be easily satisfied by many common dependence structures as shown in Ma et al. (2023).

Theorem 2. *Suppose Conditions (A4) to (A6) hold. If $h \rightarrow 0$ and $m_{k_*}^2 h \rightarrow \infty$ as $m_{k_*} \rightarrow \infty$,*

$$\hat{\pi}^\tau(U_{i,j}) \rightarrow \pi^\tau(U_{i,j}),$$

in probability uniformly for all $(i, j) \in \mathcal{H}$.

The consistency results in Theorem 2 leads to a valid data-driven procedure T-SERA as shown in the following section.

3.3 Asymptotic Error Rate Control of T-SERA

Define $\mathcal{H}_\zeta = \{(i, j) \in \mathcal{H} : |\rho_{i,j,d}| \geq (\log m_{k_*})^{-2-\zeta}, d = 1 \text{ or } 2\}$. For each $i \in [m_{k_*}]$, define $\Gamma_i(\gamma) = \{j : j \in [m_{k_*}], j \neq i, |\rho_{i,j,d}| \geq (\log m_{k_*})^{-2-\gamma}, d = 1 \text{ or } 2\}$. Let $\mathcal{H}_v = \{(i, j) \in \mathcal{H} : \frac{\rho_{i,j,1} - \rho_{i,j,2}}{(\nu_{i,j,1} + \nu_{i,j,2})^{1/2}} \geq (\log m_{k_*})^{1/2+v}\}$. This section first collects some regularity conditions and then shows the error rate control of SERA.

- (A7) Suppose there exists some constant $\zeta > 0$ such that $\sum_{(i,j) \in \mathcal{H}_\zeta} \mathbb{I}\{\theta_{i,j} = 0\} = o_p(m_{k_*}^\beta)$ for any sufficiently small constant $\beta > 0$.
- (A8) Suppose $\log m_{k_*} = o\{(nm/m_{k_*})^{1/8}\}$, and there exists some $0 < \gamma < \zeta$ such that $\max_{i \in [m_{k_*}]} |\Gamma_i(\gamma)| \asymp 1$, where ζ is defined in (A7).
- (A9) Suppose, with probability tending to 1, $\pi^\tau(U_{i,j}) \in [\varrho, 1 - \varrho]$ for some sufficiently small constant $\varrho > 0$, and has bounded first derivative with respect to $U_{i,j}$. Suppose that $\text{Var}_{\theta_{i,j}, (i,j) \in \mathcal{H}} \sum_{(i,j) \in \mathcal{H}} (\mathbf{E}_{U_{i,j}}[w(U_{i,j}) | \{\theta_{i,j}, (i,j) \in \mathcal{H}\}] \mathbb{I}\{\theta_{i,j} = 0\}) = o(m_{k_*}^4)$ where $w(U_{i,j}) = \pi^\tau(U_{i,j}) / \{1 - \pi^\tau(U_{i,j})\}$.
- (A10) Suppose there exists some $\nu, \varepsilon > 0$ such that $|\mathcal{H}_\nu| \geq [1/\{(8c_\pi)^{1/2}\alpha\} + \varepsilon](\log \log m_{k_*})^{1/2}$, where $c_\pi \approx 3.14$ is a math constant.

Condition (A7) assumes that not too many mode- k_* tensor elements have strong and exactly equal correlations/partial correlations. Condition (A8) indicates that most of the test statistics are weakly correlated with each other and Condition (A9) requires that the latent variables $\theta_{i,j}$'s are not perfectly correlated. Finally, Condition (A10) is assumed to avoid an overly conservative FDR; it requires a few hypotheses to have the standardized correlation/partial correlation difference exceeding $(\log m_{k_*})^{1/2+\nu}$. The conditions are all mild and they are similarly assumed in many high-dimensional multiple testing literatures (e.g., Liu, 2013; Xia et al., 2015, 2020; Cai et al., 2022; Ma et al., 2023).

Theorem 3. *Suppose Conditions (A1) to (A10) hold. Then, for any $\epsilon > 0$,*

$$\limsup_{m_{k_*} \rightarrow \infty} \text{FDR}^{\text{T-SERA}} \leq \alpha, \quad \text{and} \quad \lim_{m_{k_*} \rightarrow \infty} \Pr \{ \text{FDP}(\boldsymbol{\delta}^{\text{T-SERA}}) \leq \alpha + \epsilon \} = 1.$$

The above asymptotic FDP and FDR control results of T-SERA can be extended to more general cases as shown in the next section.

3.4 Generality of SERA

We emphasize that, though we mainly focus on the tensor dependence testing problem in the current article, the proposed SERA is generally applicable to many other sparse two-sample multiple testing problems as detailed below.

Suppose there are two groups of data $\mathbf{Y}_d = \{Y_{i,d}\}_{i=1}^m$, $d = 1, 2$, that follows a probability distribution $\mathcal{P}_{\beta_d, \boldsymbol{\eta}_d}$, where $\beta_d = \{\beta_{i,d} : i \in [m]\}$ denotes the parameters of interest, and $\boldsymbol{\eta}_d$ collects all the nuisance parameters. Suppose we observe two sets of independent samples, $\{\mathbf{Y}_{l,d}\}_{l=1}^{n_d}$, where n_d is the sample size for group d , and one wishes to carry out multiple hypothesis testing of

$$H_{0,i} : \beta_{i,1} = \beta_{i,2} \quad \text{versus} \quad H_{1,i} : \beta_{i,1} \neq \beta_{i,2}, \quad i \in [m]. \quad (3.4)$$

Besides the tensor problem considered in this article, (3.4) also covers a range of two-sample testing problems including detecting differential networks, identifying gene-environment interactions, etc. The following corollary shows that, if the primary and auxiliary statistics $\{(T_i, U_i), i \in [m]\}$ for (3.4) are appropriately constructed (Condition (C1) below) similarly as in (2.2) for the tensor setting, then the decision rule $\boldsymbol{\delta}^{\text{SERA}}$ obtained by applying SERA to $\{(T_i, U_i), i \in [m]\}$ can asymptotically control the FDP and FDR as well.

With slight abuse of notation, we let $\mathcal{H}_0 = \{i \in [m] : \beta_{i,1} = \beta_{i,2}\}$ for the general two-sample testing problem (3.4) and let $\beta_{i,1} = \beta_{i,2} = \beta_i$ for $i \in \mathcal{H}_0$. Let $\psi(Y_{l,i,d})$ denote the influence function of $\beta_{i,d}$ at $Y_{l,i,d}$. Let $Z_{k,i} = (n_2/n_1)\psi(Y_{l,i,1})$, for $k = l, l \in [n_1]$, and $Z_{k,i} = -\psi(Y_{l,i,2})$, for $k = n_1 + l, l \in [n_2]$.

(C1) Suppose that $n_1 \asymp n_2$, $\log m = o(n^{1/8})$ and $\mathbf{E} \left\{ \exp \left(C_3 |Z_{k,i}| / [\text{Var}\{Z_{k,i}\}]^{1/2} \right) \right\} < \infty$ for some $C_3 > 0$. Suppose that there exists some $\mu_i = (1 + o\{(\log m)^{-1}\}) \mathbf{E}(U_i)$ and $b_i = O\{(\log m)^{1/2} \beta_i\}$ that satisfies $\Pr \{ \max_{i \in \mathcal{S}} |b_i| \geq x \} \leq O(|\mathcal{S}|(1 - \Phi(x)) + m^{-1})$

uniformly in $(\log m)^{1/4} \leq x \leq (4 \log m)^{1/2}$ and $\mathcal{S} \subset [m]$, such that

$$\Pr_{H_{0,i}} \left\{ \left| T_i - b_i - \frac{\sum_{k=1}^{n_1+n_2} Z_{k,i}}{\text{Var}\{\sum_{k=1}^{n_1+n_2} Z_{k,i}\}^{1/2}} \right| \geq e_m \right\} = O(m^{-C_4}),$$

$$\Pr_{H_{0,i}} \left\{ \left| [U_i - b_i - \mu_i] - \frac{\sum_{k=1}^{n_1} Z_{k,i} - \vartheta_i \sum_{k=n_1+1}^{n_1+n_2} Z_{k,i}}{\text{Var}\{\sum_{k=1}^{n_1} Z_{k,i} - \vartheta_i \sum_{k=n_1+1}^{n_1+n_2} Z_{k,i}\}^{1/2}} \right| \geq e_m \right\} = O(m^{-C_4}),$$

for some constant $C_4 > 5$ and $e_m = o\{(\log m)^{-1/2}\}$, where $\vartheta_i = [n_1 \text{Var}\{Z_{1,i}\}] / [n_2 \text{Var}\{Z_{n,i}\}]$.

Corollary 1. *Suppose Conditions (C1), (A4), (A5') - (A10') hold. Then, for any $\epsilon > 0$,*

$$\limsup_{m \rightarrow \infty} \text{FDR}^{\text{SERA}} \leq \alpha, \quad \text{and} \quad \lim_{m \rightarrow \infty} \Pr \{ \text{FDP}(\boldsymbol{\delta}^{\text{SERA}}) \leq \alpha + \epsilon \} = 1.$$

We remark that Condition (C1) can be easily satisfied by our own construction; see Xia et al. (2020) for the guidance. Conditions (A5') to (A10') are the analogs of (A5) to (A10) for the general two-sample problem in (3.4) and are presented in detail in Section S1.3 of the Online Appendix. Therefore, the above corollary provides a general guarantee of error rate control for applying the proposed SERA to a broad range of two-sample multiple testing problems discussed above.

4 Simulation Studies

In this section, we investigate the numerical performance of the proposed T-SERA under the correlation and partial correlation scenarios in turn. In both cases, we compare T-SERA with T-BH and T-GAP, where T-BH only employs the primary tensor statistics $\{T_{i,j}\}$ in (2.2) in BH procedure (Benjamini and Hochberg, 1995) and T-GAP incorporates the statistic pairs in (2.2) in GAP procedure (Xia et al., 2020). Note that, GAP adopts the auxiliary statistics in a discrete grouping fashion and is expected to be less efficient and computationally slower. In the partial correlation scenario, we additionally compare T-SERA with two modified tests from their one-sample versions (Chen and Liu, 2019; Lyu et al., 2019) (by first constructing similar statistic pairs as in (2.2) and then applying

the newly proposed SERA), and the two tests are denoted by CL-SERA and LX-SERA, respectively. The detailed descriptions of such modifications are relegated to Sections S5.1 and S5.2 of the Online Appendix. For the proposed method, we additionally compare the data-driven T-SERA with its oracle version where the nuisances $\{\Sigma_{k,d} : k \in [K] \setminus k_*; d = 1, 2\}$ are known (denoted by T-SERA^{OR}).

4.1 Data Generation and Implementation

In both scenarios, we generate the third-order tensor (i.e., $K = 3$) samples by

$$\begin{aligned} \mathbf{y}_{1,1}, \dots, \mathbf{y}_{n_1,1} &\in \mathbb{R}^{m_1 \times m_2 \times m_3} \sim \text{Tnorm}(\mathcal{M}_1, \Sigma_{1,1} \circ \Sigma_{2,1} \circ \Sigma_{3,1}), \\ \mathbf{y}_{1,2}, \dots, \mathbf{y}_{n_2,2} &\in \mathbb{R}^{m_1 \times m_2 \times m_3} \sim \text{Tnorm}(\mathcal{M}_2, \Sigma_{1,2} \circ \Sigma_{2,2} \circ \Sigma_{3,2}), \end{aligned} \quad (4.1)$$

with $m_1 = 100, m_2 = 20, m_3 = 10$ and $n_1 = n_2 = 3$, which mimic the dimensionalities and sample sizes of the datasets in Section 5. Denote by $\mathcal{M}_d = \{\mathcal{M}_{i_1, i_2, i_3, d} : i_1 \in [m_1], i_2 \in [m_2], i_3 \in [m_3]\}$. We independently generate $\mathcal{M}_{i_1, i_2, i_3, 1} \sim 3\text{N}(0, 1)$ and $\mathcal{M}_{i_1, i_2, i_3, 2} \sim 2\text{N}(0, 1)$. Without loss of generality, let the pre-specified mode of interest $k_* = 1$.

Again, we unify the dependence structures by $\mathbf{P}_k = (\rho_{i,j})_{m_k \times m_k}$ for the correlation and partial correlation scenarios. Two structural collections of \mathbf{P}_k are considered in the following generation process. The first collection consists of three sparse structures, i.e., **Band**: $\rho_{i,i} = 1$ for $i \in [m_k]$, $\rho_{i,j} = 0.6$ for $|i - j| = 1$, $\rho_{i,j} = 0.3$ for $|i - j| = 2$ and $\rho_{i,j} = 0$ otherwise; **Hub**: $\rho_{i,i} = 1$ for $i \in [m_k]$, $\rho_{i,j} = \rho_{j,i} = 0.5$ for $i = 10(l - 1) + 1, 10(l - 1) + 2 \leq j \leq 10(l - 1) + 10$ where $1 \leq l \leq m_k/10$ and $\rho_{i,j} = 0$ otherwiseⁱ; and **Random**: $\rho_{i,i} = 1$ for $i \in [m_k]$, $\rho_{i,j} = \rho_{j,i} = \text{Uniform}(0.4, 0.8) \times \text{Bernoulli}(1, \min\{0.05, 10/m_k\})$ ⁱⁱ for $1 \leq i < j \leq m_k$ and $\rho_{i,j} = 0$ otherwiseⁱ. The second collection consists of two autoregressive (AR) structures and two moving average (MA) structures, i.e., **AR4**: $\rho_{i,j} =$

ⁱIn the implementation, we let $\mathbf{P}_k \leftarrow \mathbf{P}_k + [|\lambda_{m_k}(\mathbf{P}_k)| + 0.05]\mathbf{I}_{m_k}$ to ensure the positive definiteness.

ⁱⁱThe sampling of the two distributions is independent of each other.

$0.4^{|i-j|}$; **AR5**: $\rho_{i,j} = 0.5^{|i-j|}$; **MA3**: $\rho_{i,j} = \frac{1}{|i-j|+1}$ for $1 \leq |i-j| \leq 3$ and $\rho_{i,j} = 0$ otherwise; and **MA4**: $\rho_{i,j} = \frac{1}{|i-j|+1}$ for $1 \leq |i-j| \leq 4$ and $\rho_{i,j} = 0$ otherwise.

We then introduce the generation mechanism of mode- k dependence structures for $k \in [3]$, and we start with the correlation case. For $k = k_* = 1$, namely the mode of interest, two configurations are considered. For the first configuration, we select different structures from the first dependence collection described above for each of the two groups, for example, generate $\Sigma_{1,1}$ by **Band** and $\Sigma_{1,2}$ by **Hub**. For the second configuration, we first generate a correlation matrix $\mathbf{R}_1^{(1)} = (\rho_{i,j})$ from the first structural collection and randomly select half of the non-zero locations in its upper triangle. Then, these locations are randomly divided into two sets with equal sizes, denoted by G_1 and G_2 , and we let $\Delta_d = (\delta_{i,j}), \delta_{i,j} = \rho_{i,j}$ if $(i,j) \in G_d$ and $\delta_{i,j} = 0$ otherwise, for $d = 1, 2$. Finally, we set $\Sigma_{1,d} = \mathbf{R}_1^{(1)} + \Delta_d + (\varsigma + 0.05)\mathbf{I}_{m_1}$ for $d = 1, 2$, where $\varsigma = \lfloor \min_{d=1,2} \{ \lambda_{m_1}(\mathbf{R}_1^{(1)} + \Delta_d) \} \rfloor$, and the dependence structures of the two groups are respectively denoted by the superscripts \mathbf{G}_1 and \mathbf{G}_2 (e.g., **Band** ^{\mathbf{G}_1} , **Band** ^{\mathbf{G}_2}). For $k = 2, 3$, namely the nuisance modes, two settings from the second structural collection are considered, i.e., **AR**: generate $\Sigma_{k,1}$ and $\Sigma_{k,2}$ by **AR4** and **AR5**, respectively; **MA**: generate $\Sigma_{k,1}$ and $\Sigma_{k,2}$ by **MA3** and **MA4**, respectively. For partial correlation case, for $k = 1$, same generation mechanism above is employed while replacing $\mathbf{R}_1^{(1)}$ with $\mathbf{R}_1^{(2)}$ and replacing $\Sigma_{1,d}$ with $\Omega_{1,d}$; for $k = 2, 3$, exactly the same generation process as the correlation case is adopted.

Next, we describe the implementation details of the proposed method. We estimate the nuisances by the sample covariance matrices for simplicity and computation efficiency. The bandwidth h for estimating $\pi^\tau(U_{i,j})$ in (2.8) is selected by the `hns` function in the R package `ks`. We follow Cai et al. (2022); Ma et al. (2023) and choose τ in (2.8) as the BH threshold at the significance level 0.9. To stabilize the estimation, we truncate $\hat{\pi}^\tau(U_{i,j}) = \xi$ if $\hat{\pi}^\tau(U_{i,j}) < \xi$, and $\hat{\pi}^\tau(U_{i,j}) = 1 - \xi$ if $\hat{\pi}^\tau(U_{i,j}) > 1 - \xi$, where we set $\xi = 10^{-5}$. In addition, under the partial correlation scenario, node-wise lasso is applied to obtain

the regression coefficient estimates in Algorithm 3 and the tuning parameter is chosen following Liu (2013). All simulation results are based on 100 independent replications with significance level $\alpha = 5\%$.

4.2 FDR and Power Comparison

Table 1 collects the empirical FDR and power, in percentages, of the proposed T-SERA as well as the competing methods T-BH and T-GAP under the correlation scenario. It can be seen that the proposed T-SERA successfully controls FDR in all data generation settings. Moreover, the data-driven results are close to those of the oracle procedure T-SERA^{OR}; they both show some conservativeness which may partly attribute to the conservative approximation of $\pi(U_{i,j})$ as well as the choice of bandwidth h in (2.8). Besides, T-BH often suffers from low power, especially for the second configuration where the covariance adopts Hub or Random structures. This is because the magnitudes of entries generated by these two structures are usually very small. In comparison, T-GAP improves over T-BH because of the incorporation of the auxiliary sequence through the grouping and adjusting idea in Xia et al. (2020), while the proposed method shows additional superiority over T-GAP because T-SERA reranks the p -values by exploring the underlying sparsity structure in a continuous fashion rather than discrete grouping and thereby enjoys additional testing efficiency gain.

Table 2 presents the results for the partial correlation scenario. The comparisons of T-SERA with T-BH and T-GAP are quite similar to those in Table 1. For the two additional competing methods CL-SERA and LX-SERA, it can be seen from the table that, both approaches are less powerful than T-SERA; sometimes they cannot even compete with T-BH. Therefore, across all settings, the proposed method enjoys a superior performance compared to all four competing methods.

$\Sigma_{2,d} \& \Sigma_{3,d}$	AR						MA						
	$\Sigma_{1,1}$	Band	Hub	Random	Band ^{G₁}	Hub ^{G₁}	Random ^{G₁}	Band	Hub	Random	Band ^{G₁}	Hub ^{G₁}	Random ^{G₁}
	$\Sigma_{1,2}$	Hub	Random	Band	Band ^{G₂}	Hub ^{G₂}	Random ^{G₂}	Hub	Random	Band	Band ^{G₂}	Hub ^{G₂}	Random ^{G₂}
Empirical FDR (%)													
T-SERA ^{OR}	1.63	3.19	2.27	2.25	3.64	2.51	1.53	2.89	2.36	2.31	3.17	2.81	
T-SERA	1.53	3.10	2.09	1.94	3.31	2.33	1.48	2.99	2.28	2.16	3.46	2.94	
T-BH	4.58	4.66	4.28	4.55	3.67	5.28	4.57	4.68	4.56	4.54	4.46	2.94	
T-GAP	4.70	2.82	2.69	1.83	1.69	1.27	4.68	2.99	2.99	1.63	1.30	1.57	
Empirical Power (%)													
T-SERA ^{OR}	96.46	83.46	87.72	78.03	85.87	46.08	96.35	83.50	88.12	77.99	85.84	45.35	
T-SERA	96.37	82.80	82.60	78.15	84.93	44.85	96.28	82.87	87.71	77.64	85.60	44.70	
T-BH	89.54	58.14	70.31	45.57	5.53	1.67	89.29	57.95	70.24	46.42	5.16	1.59	
T-GAP	94.30	75.86	82.11	76.57	76.09	35.08	94.46	75.73	81.84	76.80	77.67	35.04	

Table 1: The empirical FDR and power comparison for the correlation scenario; $\alpha = 5\%$.

$\Sigma_{2,d} \& \Sigma_{3,d}$	AR						MA						
	$\Omega_{1,1}$	Band	Hub	Random	Band ^{G₁}	Hub ^{G₁}	Random ^{G₁}	Band	Hub	Random	Band ^{G₁}	Hub ^{G₁}	Random ^{G₁}
	$\Omega_{1,2}$	Hub	Random	Band	Band ^{G₂}	Hub ^{G₂}	Random ^{G₂}	Hub	Random	Band	Band ^{G₂}	Hub ^{G₂}	Random ^{G₂}
Empirical FDR (%)													
T-SERA ^{OR}	0.95	2.16	1.48	2.07	3.26	2.29	0.94	2.30	1.66	2.34	3.24	1.92	
T-SERA	2.31	4.60	2.55	3.46	5.09	3.08	2.77	5.24	2.92	3.94	5.68	3.32	
T-BH	5.58	6.76	5.13	5.47	5.18	4.02	5.61	7.00	5.63	5.37	7.15	5.25	
T-GAP	6.02	4.05	3.28	2.73	4.67	1.62	6.41	4.34	3.75	3.10	4.75	1.50	
CL-SERA	0.93	1.33	0.54	3.71	4.66	2.99	1.78	0.98	0.82	2.99	2.76	1.88	
LX-SERA	1.42	2.57	1.36	1.66	2.84	1.35	1.09	2.30	0.84	1.09	2.99	5.94	
Empirical Power (%)													
T-SERA ^{OR}	96.56	88.67	90.79	85.50	95.42	58.98	96.65	88.66	91.27	85.41	96.27	58.06	
T-SERA	96.66	87.32	90.14	83.57	96.04	56.69	96.74	87.24	90.71	82.79	95.96	56.29	
T-BH	92.88	67.82	76.13	56.14	38.89	4.80	92.93	67.95	76.78	56.86	38.58	5.18	
T-GAP	95.16	81.93	85.84	82.55	90.71	48.10	95.21	81.80	86.04	82.07	90.58	47.53	
CL-SERA	87.15	51.65	62.00	65.37	46.09	27.96	83.20	57.46	61.09	61.77	56.16	18.10	
LX-SERA	80.83	58.06	66.91	60.05	20.56	9.12	69.09	38.83	53.79	52.42	5.20	1.54	

Table 2: The empirical FDR and power comparison for the partial correlation scenario; $\alpha = 5\%$.

5 Real Data Analysis

In this section, we investigate the performance of the proposed method on two real datasets, an international trade dataset for detecting correlation alteration of commodity

types, and a climate dataset for detecting partial correlation alteration of spatial locations in US. Significance levels are set as $\alpha = 5\%$ in both studies.

5.1 Example of Correlation Comparison

The first dataset consists of monthly imports (CIF value) of 97 commodity types over 30 countries from the year 2015 to 2022, and is available at the UN Comtrade website <https://comtradeplus.un.org>. Data from each year serves as an observation, which is a $97 \times 30 \times 12$ tensor. Such trade data have been well studied in the literatures, for example, in correlation estimation (Hoff, 2011) and tensor extrapolation (Schosser, 2022). Following the spirit of Hoff (2011), the scientific interest in this section is to detect the correlation alteration of the commodity mode (i.e., $k_* = 1$), before and after *COVID-19 pandemic* hit in December 2019 (Page et al., 2021). After adopting the pre-processing method in Leng and Tang (2012) and Chen and Liu (2019) that reduces the potential serial correlations among the observations, the first group of the processed dataset consists of the lag-one differential tensor observations from 2016 to 2019, and the second group consists of those from 2020 to 2022. The complete lists of 97 commodity types and 30 countries are collected in Section S6.1 of the Online Appendix.

Before conducting the analysis, it is crucial to verify the separability assumption in the covariance structure. Specifically, we adopt the bootstrap method proposed in Aston et al. (2017) and apply their test to each of the mode- k matricization, $k \in [3]$, for both groups respectively. The results suggest the acceptance of the separability assumption. Next, we apply T-BH, T-GAP and T-SERA to the dataset and they yield a rejection of 64, 92, and 98 respectively, out of a total of 4656 hypotheses. Besides, the altered correlations among commodities found by T-SERA covers 98.4% of those found by T-BH and 97.8% of those found by T-GAP. Together with our simulation studies, it suggests that the proposed T-SERA manages to achieve the best power. Note that from an economic

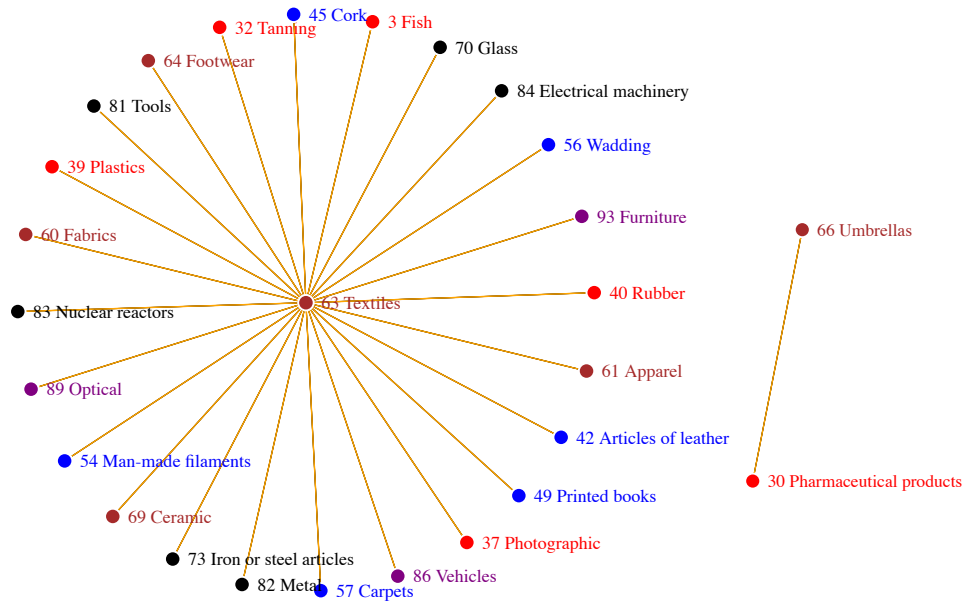


Figure 1: Top 25 correlation alterations found by T-SERA in the trade example; $\alpha = 5\%$. Each node is a commodity type named by its index and its first phrase; see commodity descriptions in Table S1 in Section S6.1 of the Online Appendix.

perspective, imports of substitutable commodities may have a high negative correlation, while imports of complementary commodities may have a positive correlation. However, the COVID-19 pandemic greatly impacts the global economy. For instance, countries may wish to shrink their global demands and seek for localization (Rajput et al., 2021). Such a shift may result in a reconstruction of the commodity market and an alteration of the import correlation. To facilitate visualization, in Figure 1 we picture the top 25 detected alterations by T-SERA according to its weighted p -values. We observe that 24 out of those 25 top findings are related to the commodity type “Textiles”, which agrees with the literature conclusion that the COVID-19 pandemic impacts the international trades of the textile and fashion industry (Blancheton, 2021; Kanupriya, 2021; Arania et al., 2022; Haukkala et al., 2023).

5.2 Example of Partial Correlation Comparison

The second dataset consists of monthly measurements of 17 meteorological factors over 125 locations in US from the year 1990 to 1996, and is available at the USC Melady Lab website <https://viterbi-web.usc.edu/~liu32/data.html>. The locations are pictured as the red dots in Figure 2 according to their longitudes and latitudes; the complete list of 125 location coordinates and 17 meteorological factors are collected in Section S6.2 of the Online Appendix. In this application, data from each year serves as an observation, which is a $125 \times 17 \times 12$ tensor. This dataset has been employed in Chen and Liu (2019) for estimating the support of the precision matrices, and in Lozano et al. (2009) for extreme value modeling. Following the spirit of Chen and Liu (2019), the scientific interest in this section is to detect partial correlation (conditional dependence) alteration of locations (i.e., $k_* = 1$) before and after the *1994 North American cold wave* in January 1994 (Ludlum, 1994). Similarly, we apply the lag-one pre-processing step as in Section 5.1 to make the samples independent. That is, the first group consists of the lag-one differential tensor observations from 1991 to 1993, and the second group consists of those from 1994 to 1996. In contrast, Chen and Liu (2019) merges the monthly observations into an annual dataset and considers a one-sample matrix-valued inference with dimension 125×17 .

Same as Section 5.1, we first verify the separability by Aston et al. (2017) and the assumption is affirmed. Next, we apply T-BH, T-GAP, CL-SERA, LX-SERA and the proposed T-SERA to the dataset. These five methods yield a rejection of 939, 958, 1, 0, and 1303 respectively, out of a total of 7750 hypotheses. Besides, the altered partial correlations found by T-SERA cover all those found by T-BH and T-GAP. In addition, the tests by Chen and Liu (2019) and Lyu et al. (2019) suffer from trivial power, which may due to the over-correction of variances in their procedures (and thereby a decreasing signal-noise ratio) when the underlying nuisance covariances are dense. In summary, it again suggests that

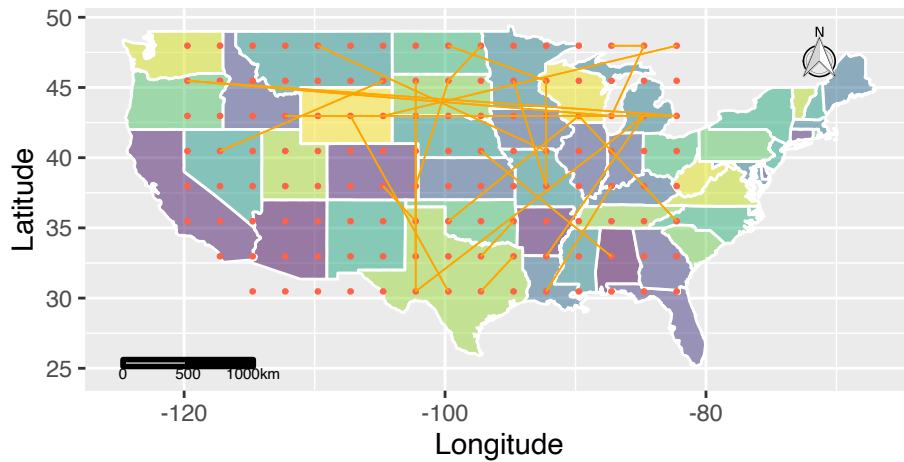


Figure 2: Top 25 partial correlation alterations found by T-SERA in the climate example; $\alpha = 5\%$; see location details in Table S2 in Section S6.2 of the Online Appendix.

the proposed T-SERA achieves the best performance. Finally, we visualize in Figure 2 the top 25 altered partial correlations found by T-SERA according to its weighted p -values. It is observed that the altered partial correlations are mostly detected in Midwestern regions of US. Such phenomenon is consistent with the historical fact that the extreme weather in 1994 mainly occurred in the Midwestern US (Schmidlin, 1997).

References

- Arania, F., Putri, I. M., and Saifuddin, M. (2022). The impact of Covid-19 on textile and fashion industries: the economic perspective. *Journal of Marketing Innovation (JMI)*, 2(1).
- Aston, J. A. D., Pigoli, D., and Tavakoli, S. (2017). Tests for separability in nonparametric covariance operators of random surfaces. *The Annals of Statistics*, 45(4):1431–1461.
- Bagchi, P. and Dette, H. (2020). A test for separability in covariance operators of random surfaces. *The Annals of Statistics*, 48(4):2303–2322.
- Benjamini, Y. and Hochberg, Y. (1995). Controlling the false discovery rate: a practical and powerful approach to multiple testing. *Journal of the Royal Statistical Society: Series B (Statistical Methodology)*, 57(1):289–300.
- Bickel, P. J. and Levina, E. (2008). Regularized estimation of large covariance matrices. *The Annals of Statistics*, 36(1):199–227.
- Blancheton, B. (2021). French fashion and textile during covid-19. once again, flying to high quality and innovation to survive. *Fashion and Textiles*, 8(1):1–13.
- Cai, T. and Liu, W. (2011). Adaptive thresholding for sparse covariance matrix estimation. *Journal of the American Statistical Association*, 106(494):672–684.
- Cai, T. T. and Liu, W. (2016). Large-scale multiple testing of correlations. *Journal of the American Statistical Association*, 111(513):229–240.
- Cai, T. T., Sun, W., and Wang, W. (2019). Covariate-assisted ranking and screening for large-scale two-sample inference. *Journal of the Royal Statistical Society: Series B (Statistical Methodology)*, 81(2):187–234.

- Cai, T. T., Sun, W., and Xia, Y. (2022). LAWS: A locally adaptive weighting and screening approach to spatial multiple testing. *Journal of the American Statistical Association*, 117(539):1370–1383.
- Chen, X. and Liu, W. (2019). Graph estimation for matrix-variate gaussian data. *Statistica Sinica*, 29(1):479–504.
- Chen, X., Yang, D., Xu, Y., Xia, Y., Wang, D., and Shen, H. (2023). Testing and support recovery of correlation structures for matrix-valued observations with an application to stock market data. *Journal of Econometrics*, 232(2):544–564.
- Constantinou, P., Kokoszka, P., and Reimherr, M. (2017). Testing separability of space-time functional processes. *Biometrika*, 104(2):425–437.
- De Lathauwer, L., De Moor, B., and Vandewalle, J. (2000). A multilinear singular value decomposition. *SIAM journal on Matrix Analysis and Applications*, 21(4):1253–1278.
- Efron, B. (2009). Are a set of microarrays independent of each other? *The annals of applied statistics*, 3(3):922.
- Haukkala, T., Niinimäki, K., and Turunen, L. L. M. (2023). Fashion in turmoil: impact of the COVID-19 pandemic on Finland’s textile and fashion industry. *Sustainability: Science, Practice and Policy*, 19(1):2173424.
- He, S., Yin, J., Li, H., and Wang, X. (2014). Graphical model selection and estimation for high dimensional tensor data. *Journal of Multivariate Analysis*, 128:165–185.
- Hoff, P. D. (2011). Separable covariance arrays via the tucker product, with applications to multivariate relational data. *Bayesian Analysis*, 6(2):179–196.
- Hoff, P. D. (2015). Multilinear tensor regression for longitudinal relational data. *The Annals of Applied Statistics*, 9(3):1169.

- Hore, V., Vinuela, A., Buil, A., Knight, J., McCarthy, M. I., Small, K., and Marchini, J. (2016). Tensor decomposition for multiple-tissue gene expression experiments. *Nature Genetics*, 48(9):1094–1100.
- Hornstein, M., Fan, R., Shedden, K., and Zhou, S. (2019). Joint mean and covariance estimation with unreplicated matrix-variate data. *Journal of the American Statistical Association*, 114(526):682–696.
- Kanupriya (2021). COVID-19 and the Indian textiles sector: Issues, challenges and prospects. *Vision*, 25(1):7–11.
- Kolda, T. G. (2006). Multilinear operators for higher-order decompositions. Technical Report SAND2006-2081, Sandia National Laboratories.
- Leng, C. and Tang, C. Y. (2012). Sparse matrix graphical models. *Journal of the American Statistical Association*, 107(499):1187–1200.
- Li, A. and Barber, R. F. (2019). Multiple testing with the structure-adaptive Benjamini–Hochberg algorithm. *Journal of the Royal Statistical Society: Series B (Statistical Methodology)*, 81(1):45–74.
- Li, L. and Zhang, X. (2017). Parsimonious tensor response regression. *Journal of the American Statistical Association*, 112(519):1131–1146.
- Liang, Z., Cai, T. T., Sun, W., and Xia, Y. (2023). Locally adaptive algorithms for multiple testing with network structure, with application to genome-wide association studies. *arXiv preprint arXiv:2203.11461*.
- Liu, W. (2013). Gaussian graphical model estimation with false discovery rate control. *The Annals of Statistics*, 41(6):2948–2978.

- Liu, W. (2014). Incorporation of sparsity information in large-scale multiple two-sample t tests. *arXiv preprint arXiv:1410.4282*.
- Lozano, A. C., Li, H., Niculescu-Mizil, A., Liu, Y., Perlich, C., Hosking, J., and Abe, N. (2009). Spatial-temporal causal modeling for climate change attribution. In *Proceedings of the 15th ACM SIGKDD International Conference on Knowledge Discovery and Data Mining*, pages 587–596.
- Ludlum, D. M. (1994). January 1994. *Weatherwise*, 47(2):44–49.
- Lyu, X., Sun, W. W., Wang, Z., Liu, H., Yang, J., and Cheng, G. (2019). Tensor graphical model: Non-convex optimization and statistical inference. *IEEE Transactions on Pattern Analysis and Machine Intelligence*, 42(8):2024–2037.
- Ma, L., Xia, Y., and Li, L. (2023). NAPA: Neighborhood-assisted and posterior-adjusted two-sample inference. *arXiv preprint arXiv:2201.10043*.
- Manceur, A. M. and Dutilleul, P. (2013). Maximum likelihood estimation for the tensor normal distribution: Algorithm, minimum sample size, and empirical bias and dispersion. *Journal of Computational and Applied Mathematics*, 239:37–49.
- Min, K., Mai, Q., and Zhang, X. (2022). Fast and separable estimation in high-dimensional tensor gaussian graphical models. *Journal of Computational and Graphical Statistics*, 31(1):294–300.
- Nadaraya, E. A. (1964). On estimating regression. *Theory of Probability & Its Applications*, 9(1):141–142.
- Nzabanita, J., von Rosen, D., and Singull, M. (2015). Maximum likelihood estimation in the tensor normal model with a structured mean.

- Page, J., Hinshaw, D., and McKay, B. (2021). In Hunt for Covid-19 Origin, Patient Zero Points to Second Wuhan Market—The man with the first confirmed infection of the new coronavirus told the WHO team that his parents had shopped there. *The Wall Street Journal*, 26.
- Pan, Y., Mai, Q., and Zhang, X. (2019). Covariate-adjusted tensor classification in high dimensions. *Journal of the American Statistical Association*, 114(527):1305–1319.
- Rajput, H., Changotra, R., Rajput, P., Gautam, S., Gollakota, A. R., and Arora, A. S. (2021). A shock like no other: coronavirus rattles commodity markets. *Environment, Development and Sustainability*, 23:6564–6575.
- Schmidlin, T. W. (1997). Recent state minimum temperature records in the midwest. *Bulletin of the American Meteorological Society*, 78(1):35–40.
- Schosser, J. (2022). Tensor extrapolation: Forecasting large-scale relational data. *Journal of the Operational Research Society*, 73(5):969–978.
- Singull, M., Ahmad, M. R., and von Rosen, D. (2012). More on the kronecker structured covariance matrix. *Communications in Statistics-Theory and Methods*, 41(13-14):2512–2523.
- Stolp, H., Ball, G., So, P.-W., Tournier, J.-D., Jones, M., Thornton, C., and Edwards, A. (2018). Voxel-wise comparisons of cellular microstructure and diffusion-MRI in mouse hippocampus using 3D Bridging of Optically-clear histology with Neuroimaging Data (3D-BOND). *Scientific Reports*, 8(1):4011.
- Tsiligkaridis, T., Hero III, A. O., and Zhou, S. (2013). On convergence of kronecker graphical lasso algorithms. *IEEE Transactions on Signal Processing*, 61(7):1743–1755.

- Tucker, L. R. (1966). Some mathematical notes on three-mode factor analysis. *Psychometrika*, 31(3):279–311.
- Wang, X., Yang, L. T., Kuang, L., Liu, X., Zhang, Q., and Deen, M. J. (2019). A tensor-based big-data-driven routing recommendation approach for heterogeneous networks. *IEEE Network*, 33(1):64–69.
- Watson, G. S. (1964). Smooth regression analysis. *Sankhyā: The Indian Journal of Statistics, Series A*, 26(4):359–372.
- Xia, Y. (2017). Testing and support recovery of multiple high-dimensional covariance matrices with false discovery rate control. *Test*, 26(4):782–801.
- Xia, Y., Cai, T., and Cai, T. T. (2015). Testing differential networks with applications to the detection of gene-gene interactions. *Biometrika*, 102(2):247–266.
- Xia, Y., Cai, T. T., and Sun, W. (2020). GAP: A General Framework for Information Pooling in Two-Sample Sparse Inference. *Journal of the American Statistical Association*, 115(531):1236–1250.
- Xia, Y. and Li, L. (2017). Hypothesis testing of matrix graph model with application to brain connectivity analysis. *Biometrics*, 73(3):780–791.
- Xia, Y. and Li, L. (2019). Matrix graph hypothesis testing and application in brain connectivity alternation detection. *Statistica Sinica*, 29(1):303–328.
- Xu, P., Zhang, T., and Gu, Q. (2017). Efficient algorithm for sparse tensor-variate gaussian graphical models via gradient descent. In *Artificial Intelligence and Statistics*, pages 923–932. PMLR.
- Yin, J. and Li, H. (2012). Model selection and estimation in the matrix normal graphical model. *Journal of Multivariate Analysis*, 107:119–140.

- Zahn, J. M., Poosala, S., Owen, A. B., Ingram, D. K., Lustig, A., Carter, A., Weeraratna, A. T., Taub, D. D., Gorospe, M., Mazan-Mamczarz, K., et al. (2007). AGEMAP: a gene expression database for aging in mice. *PLoS Genetics*, 3(11):e201.
- Zhang, Y., Bi, X., Tang, N., and Qu, A. (2021). Dynamic tensor recommender systems. *The Journal of Machine Learning Research*, 22(1):3032–3066.
- Zhang, Y., Shen, W., and Kong, D. (2022). Covariance estimation for matrix-valued data. *Journal of the American Statistical Association*, 0(0):1–12.
- Zhou, J., Sun, W. W., Zhang, J., and Li, L. (2023). Partially observed dynamic tensor response regression. *Journal of the American Statistical Association*, 118(541):424–439.
- Zhou, S. (2014). Gemini: Graph estimation with matrix variate normal instances. *The Annals of Statistics*, 42(2):532–562.
- Zhu, Y. and Li, L. (2018). Multiple matrix gaussian graphs estimation. *Journal of the Royal Statistical Society: Series B (Statistical Methodology)*, 80(5):927–950.